WPHCD-PR(18) 20916

T Bucko et al.

Surface reconstruction affects the work function of molybdenum (001) and its temperature dependence

Preprint of Paper to be submitted for publication in
Journal of Physics: Condensed Matter

This work has been carried out within the framework of the EUROfusion Consortium and has received funding from the Euratom research and training programme 2014-2018 under grant agreement No 633053. The views and opinions expressed herein do not necessarily reflect those of the European Commission.

On the work function of the surface Mo(001) and its temperature dependence: an ab-initio molecular dynamics study

Tomáš Bučko,[1,2,*] Michal Novotný,[1] and Ivan Černušák[1]

[1]*Department of Physical and Theoretical Chemistry, Faculty of Natural Sciences, Comenius University in Bratislava, Ilkovičova 6, SK-84215 Bratislava, SLOVAKIA*

[2]*Institute of Inorganic Chemistry, Slovak Academy of Sciences, Dubravska cesta 9, SK-84236 Bratislava, SLOVAKIA*

(Dated: October 19, 2018)

Abstract

Ab-initio molecular dynamics simulations in NVT ensemble have been performed to investigate the finite temperature structure of the Mo(001) surface and its effect on work function (ϕ). In accord with previous experimental and theoretical work, our simulations predict that a termination with a stable reconstruction pattern is formed at T=123 K. This pattern vanishes when temperature is increased to 423 K or 623 K and a disordered surface phase is formed whose time average corresponds to a bulk-like termination. Our results demonstrate that the surface relaxation is an important factor contributing to thermal variation of ϕ. At the lowest temperature, at which a stable reconstruction pattern is formed, the work function is found to increase by $\sim$0.23 eV compared to relaxed unreconstructed surface. The disappearance of stable reconstruction pattern at elevated temperatures leads to a decrease of ϕ by $\sim$0.07 eV. In contrast, the values computed for a non-reconstructing surface Mo(110) at T=123 K, 423 K and 623 K are found to be nearly identical to the zero temperature value, which is a consequence of restricted atomic motion due to high packing density in this surface.

PACS numbers: 65.40.gh, 68.35.bd, 68.35.Md

* bucko19@uniba.sk

I. INTRODUCTION

The work function (ϕ) represents the minimum work needed to shift an electron from the interior of a solid to a point outside the crystal separated from the surface by a distance that is large on the atomic scale but small compared with the linear dimensions of the crystal [1]. Although this physical property is an important characteristics of a metal surface, its thermal dependence is not yet well understood. Due to complicated measurements, the relevant experimental data are rather scarce, and often contradictory [2]. Typically, the thermal coefficient of work function ($K = d\phi/dT$) takes a value of order of k_B and its sign depends on the particular face of material. As the ingredients contributing to K, thermal lattice expansion and atomic vibrations have been identified in previous theoretical work of Kiejna [3], and these two factors tend to cancel each other to some extent. The theoretical analysis [3] also revealed that absolute value of the thermal coefficient of work function for a given metal decreases with an increase of the packing density in the plane.

Being motivated by the use of molybdenum as a construction material of the negative hydrogen ion sources that are developed for the needs of future nuclear fusion devices [4], in this work we investigate the temperature dependence of ϕ of the surface Mo(001) by means of zero- and finite-temperature ground-state DFT simulations. The work function is indeed a key characteristics of the H^- source surface as its value affects the yield of ions in the electron extraction processes [5]. As the typical operating temperature in our target application is as high as 423 K [5], the understanding of thermal effect on the work function is of great interest. Although the literature is rather rich in reports on theoretical investigations of diverse low-index Mo surfaces with and without adatoms [6–12], the ϕ vs. T dependence has, to the best of our knowledge, never been studied.

Another reason for choosing the Mo(001) surface as the model system in this study is the fact that it reconstructs reversibly and continuously (i.e. the surface phase transition is described as a second order process [13]) into a stable c($7\sqrt{2} \times \sqrt{2}$)R45° pattern (see Fig. 1(e)) at low temperature, as shown in previous experimental [13–16] and empirical force-field molecular dynamics [17] studies. Although some aspects of this reconstruction have been studied in previous ab initio works [18, 19], its effect on the work function has not yet been investigated. Furthermore, the surface termination of Mo(001) is temperature dependent: the stable surface reconstruction pattern vanishes at $T_c \approx 250$ K [14] and a

bulk-like termination p(1 × 1) (see Fig. 1(a)) prevails at higher temperatures [17]. In this work, we shall demonstrate for the first time that the surface reconstruction affects the value of work function significantly and it also plays a role in temperature dependence of ϕ. This paper is organized as follows. In Sec. II, the methodology used in our simulations is introduced. The zero- and finite-temperature results for the surface Mo(001) are discussed in Sec. III A and III B, respectively. These results are put into contrast with those for the non-reconstructing surface Mo(110) in Sec. III C. Finally, conclusions are given in Sec. IV.

II. METHODOLOGY

The calculations have been performed using the periodic density-functional theory (DFT) code Vienna Ab-initio Simulation Package (VASP) [20–23] in version 5.4.4. The Kohn-Sham equations have been solved variationally in a plane-wave basis set using the projector-augmented-wave (PAW) method of Blöchl [24], as adapted by Kresse and Joubert [25]. The Perdew, Burke, and Ernzerhof (PBE) exchange-correlation functional in the generalized gradient approximation proposed by Perdew et al. [26] was used. The plane-wave cutoff of 224.6 eV was used in all calculations presented in this work which is a default for the PAW pseudopotential of Mo (version v.54, PAW_PBE Mo 08Apr2002) used in our calculations (six valence electrons). In relaxations and all work function calculations, the two-dimensional Brillouin zone has been sampled by a mesh of $M_1 \times M_2$ k-points, whereby the numbers M_1 and M_2 have been chosen so that $(M_i\,|\boldsymbol{a}_i|)^{-1} \approx 0.01$ Å^{-1} for the lattice vectors $\boldsymbol{a}_1$ and $\boldsymbol{a}_2$ parallel with the surface. The convergence criterion for the electronic self-consistency cycle, measured by the change in the total energy between successive iterations, was set to 10^{-6} eV/cell. The conjugate-gradient algorithm [27] has been employed in relaxations of atomic positions. The relaxations have been conducted until the difference in the total forces acting on each atom were smaller than 5×10^{-3} eV/Å. The equilibrium lattice constant (a) of body centered cubic Mo used to build all structural models employed in this work has been determined by fitting the energy versus volume dependence, computed in a series of single point calculations, by Murnaghan equation of state [28]. The computed value of a =3.150 Å is found to be in a good agreement with experiment [29] (3.144 Å) as well as with previous DFT calculations (3.150 Å) [10, 12]. The surface energy (γ) has been computed using the

following formula:

$$\gamma = \frac{E(\text{slab}) - NE(\text{bulk})}{2A}, \tag{1}$$

where E(slab) is the energy of relaxed slab, E(bulk) is the ground-state bulk energy per atom, N is the number of atoms in slab and A is the area per a single surface of slab. The work function has been determined as follows [30]:

$$\phi = E_{\text{vac}} - E_{\text{F}}, \tag{2}$$

where E_{vac} and E_{F} are the vacuum level energy and the Fermi energy, respectively.

In the ab-initio molecular dynamics (MD) simulations, the simulation temperature was controlled using the Andersen thermostat [31] with a collision frequency of 0.01 fs^{-1}. Classical equations of motion have been integrated using the leap-frog algorithm [32] with a time step of 2 fs. The total length of trajectories was 50 ps, whereby the initial period of 5 ps was considered as equilibration and the corresponding data were discarded from calculations of time averages. In order to accelerate the MD simulations, the k-points mesh was reduced so that $(M_i\,|\boldsymbol{a}_i|)^{-1} \approx 0.03$ Å^{-1} (i.e. a grid of 2×2 k-points was used for a 5×5 slab model, see Sec. III B).

The Supplemental Material [33] contains the following additional information relevant to this section: (i) in Sec.SII it is shown that increasing the plane wave cutoff has negligible effect on the computed values of γ and ϕ presented in Sec. III A, (ii) the fact that the reduced k-points mesh employed in the MD simulations does not introduce a significant bias into our configuration space sampling is demonstrated in Sec.SV, (iii) the structural input files for all relaxed structures discussed in Sec. III A, as well as the corresponding k-points grids used in calculations are provided in Sec. SI (these structural input files are also provided as electronic supplemental information, see the file SI_files.tgz).

III. RESULTS AND DISCUSSION

A. Zero-temperature simulations of Mo(001)

We start our discussion by analyzing the effect of reconstruction on work function of Mo(001) at T=0 K. To this end, atomic relaxations of slab models with nine Mo layers and vacuum corresponding to the width of 13 bulk layers (i.e. 20.475 Å) have been conducted.

The following surface terminations previously discussed in literature [18, 19] have been considered (see Fig. 1): p(1×1) corresponds to unreconstructed bulk like termination, c($7\sqrt{2} \times \sqrt{2}$)R45° represents the experimentally observed low temperature pattern [14–16], and terminations c($\sqrt{2} \times \sqrt{2}$)R45°, c($3\sqrt{2} \times \sqrt{2}$)R45°, and c($5\sqrt{2} \times \sqrt{2}$)R45° are analogues of c($7\sqrt{2} \times \sqrt{2}$)R45° differing in the number of zig-zag rows separated by straight misfit lines of atoms (*vide infra*). For the unrelaxed unreconstructed surface (p(1×1)), in which all separations between the neighboring (001) planes are the same as in bulk (i.e. $a/2$), the computed values of work function and surface energy are 3.92 eV and 3.52 J/m^2, respectively. Let us define a relative average spacing between layers m and n ($\Delta_{m,n}$) as follows:

$$\Delta_{m,n} = \frac{\bar{d}_{m,n} - d_0}{d_0}, \tag{3}$$

where $\bar{d}_{m,n}$ is the average distance between layers m and n and $d_0 = a/2$ is the separation between two neighboring (001) planes in bulk. As evident from the data presented in Tab. I, the relaxation of surface atoms (without reconstruction) of the structure p(1×1) leads to a significant reduction (-13.4%) of the interlayer spacing between two topmost layers ($\Delta_{1,2}$) followed by a modest (3.7%) expansion of the spacing between the layers 2 and 3. The relaxation also leads to a significant decrease of γ to 3.259 J/m^2. The computed work function, however, turns out to be almost insensitive to these structural changes and the value computed for the relaxed structure (3.88 eV) differs only modestly from that determined for the unrelaxed slab. We note that our results for γ and ϕ are in good agreement with the previous theoretical reports [12, 34, 35] employing the same simulation method as we used in this work, see Tab. II.

As evident from Tab. I, the surface reconstruction tends to reduce the absolute values of $\Delta_{1,2}$ and $\Delta_{2,3}$ observed in the relaxed p(1×1) structure. The change in the spacing between the subsequent layers is virtually negligible and this result is independent of the surface termination. In Tab. III, the average parallel displacements of atoms in layer n (δ_n) with respect to positions of atoms in a bulk-like surface arrangement are compiled, which we define as follows:

$$\delta_n = \frac{1}{N_n} \sum_{i=1}^{N_n} \sqrt{(x_i - x_{0,i})^2 + (y_i - y_{0,i})^2}, \tag{4}$$

where x_i and y_i are the Cartesian $x-$ and $y-$ coordinates of atom i, $x_{0,i}$ and $y_{0,i}$ are those for the bulk-like surface structure, the sum is over all N_n atoms in the layer n, and it is assumed that the direction [001] is parallel with the Cartesian coordinate z. As expected,

the largest δ_n is found for the first layer of reconstructed surfaces. The value of δ_2 is an order of magnitude smaller than δ_1, and the average parallel atomic displacements for all remaining layers are negligible. Note that by eq. 4, δ_n=0 for all layers of unreconstructed surfaces with termination p(1 × 1). Combined with the results presented in Tab. I, we conclude that a significant atomic rearrangement due to the relaxation and reconstruction occurs only within two topmost layers of Mo(001). This result justifies the use of a relatively thin slab model (5 layers) in our MD simulations (see Sec. III B).

The common feature of all reconstruction patterns considered in this work is the presence zig-zag rows formed by the unsaturated surface atoms in attempt to shorten their mutual distance from 3.15 Å to approximately the bulk nearest-neighbour (NN) spacing [18, 36] (2.73 Å). As shown in Fig. 1, the NN spacing within a single zig-zag row formed in surfaces with different terminations varies in a relatively narrow interval of 2.77 Å to 2.82 Å. This shortening of bonds between pairs of atoms is accompanied by elongation of distances with other neighbors which are stretched from 3.15 Å to 3.31-3.52 Å and this effect prevents a further surface relaxation [18]. It has been shown by Roelofs et al. [18] that the formation of unpaired (misfit) rows of atoms separating the zig-zag rows in the c($3\sqrt{2}\times\sqrt{2}$)R45°, c($5\sqrt{2}\times\sqrt{2}$)R45°, and c($7\sqrt{2}\times\sqrt{2}$)R45° patterns has a stabilizing effect as it leads to a decrease of the nearest neighbor distances within the plane (the nearest interatomic separation between the zigzag and the misfit rows is 3.31−3.42 Å while that between two zig-zag rows is ∼3.52 Å, see Fig. 1). In agreement with theoretical work of Haas et al. [19], our results summarized in Tab. II suggest that the reconstruction always leads to a stabilization (i.e. decrease in γ) of the (001) surface but the differences between various reconstruction patterns are very small. The model with the termination c($5\sqrt{2}\times\sqrt{2}$)R45° appears to be slightly more stable than the experimentally observed surface pattern c($7\sqrt{2}\times\sqrt{2}$)R45° but the corresponding difference in γ is only 0.003 J/m^2. The difference in potential energy between the most stable model c($5\sqrt{2}\times\sqrt{2}$)R45° and the relaxed unreconstructed slab p(1 × 1) at T=0 K is only 0.0086 eV/atom, i.e. close to the $k_B T$ term for T≈100 K. One can therefore expect that the likelihood of breaking of the Mo-Mo bonds formed in the reconstructed surfaces will increase with increasing temperature and the reconstructed termination should eventually become unstable at sufficiently high T. We shall demonstrate in Sec. III B that this is indeed the case. Despite the relatively modest structural rearrangement and the corresponding energy lowering, the effect of reconstruction on the computed value of ϕ is surprisingly

large: the work function increases from 3.88 eV for unreconstructed surface to ∼4.11 eV for the reconstructed surfaces, improving thus the agreement with experiment 4.46±0.11 [37]). One could therefore expect that ϕ should decrease by ∼0.2 eV when T is increased from 0 K to T$\gg$T$_c$. As we shall see in Sec. III B, such a naive estimate is only qualitatively correct and the actual decrease of ϕ with T is much smaller.

B. Finite-temperature simulations of Mo(001)

Altogether, the reconstruction has a significant effect on work function of Mo(001) but, as already mentioned, this reconstruction is temperature dependent and it vanishes at T>T$_c$ ≈250 K [14]. We have investigated this effect by means of Born-Oppenheimer ab initio molecular dynamics (MD) simulations in the NVT ensemble. As shown in Sec. III A, a substantial rearrangement of atoms in the Mo(001) surface occurs only in two uppermost layers. In order to reduce the simulation time of the MD calculations, it is therefore legitimate to use a model containing a reduced number of layers. In our MD simulations, a 5×5 model with 5 layers (containing 125 atoms) has been used, see Fig. 2(a). This model has been prepared as a 5×5 multiple of the relaxed slab p(1 × 1) from which four bottommost layers have been removed. The atomic positions in two bottommost layers (originally located in the center of the slab with nine layers) were fixed whereas the atoms in the remaining three layers were allowed to move in MD. For all MD simulations reported in this work, the average temperatures of all individual layers of free atoms have been found to differ from the target T by less than 1%. We note that our structural model allows for the energetically most favourable reconstruction c($5\sqrt{2} \times \sqrt{2}$)R45° but as the experimentally observed termination c($7\sqrt{2} \times \sqrt{2}$)R45° is similar in many aspects (see Sec. III A), we expect that the results presented in this section are valid also for this latter structure. As the initial configuration, the unreconstructed surface with the width of vacuum regime of 17.625 Å has been used in all simulations. A dipole correction [38] was applied for the direction perpendicular to the surface.

Three different simulation temperatures have been considered: T$_1$=123 K is well below the T$_c$, T$_2$=423 K is above T$_c$ and corresponds to a typical operating temperature in the H$^-$ source [5] being developed for the needs of the fusion device ITER [39], and T$_3$=623 K is well above T$_c$. The average interlayer separation varies only modestly with T (see Sec.SIII in the

Supplemental Material [33])), which is a consequence of a low thermal expansion of Mo (the linear thermal expansion coefficient of Mo is only $4.8{\cdot}10^{-6}$ K^{-1} [40]). Fig. 3 shows the radial distribution functions (RDF) determined for the first and the second layer of Mo(001). As expected, the RDF computed for the first layer at T_1 differs significantly from those determined for other two temperatures. In particular, the nearest neighbour peaks centered at ∼2.80 Å and ∼3.44 Å, corresponding to the NN distances between atoms within a single zig-zag row and distances between atoms in two neighboring rows, respectively (see Fig. 1), are well separated at T_1. Indeed, the average and also all instantaneous structures obtained from this simulation are very similar to the relaxed slab with termination $c(5\sqrt{2} \times \sqrt{2})R45°$ (see Fig.S1 and animation Mo001_123K.mpg provided as Supplemental Material [33]). At T_2 and T_3, the two NN peaks merge together to form a single broad band centered at the bulk-like value of ∼3.15 Å. Interestingly, the shape of RDF is rather similar for both temperatures. These results indicate that the zig-zag rows found in all reconstructed patterns are no longer stable at elevated temperatures. Although the average structures determined from the MD simulations performed at T_2 and T_3 correspond to the unreconstructed bulk-like termination, we emphasize that every instantaneous structure generated by MD is very different from the ideal $p(1 \times 1)$ termination (see Fig.S1 and animations Mo001_423K.mpg and Mo001_623K.mpg provided as Supplemental Material [33]). Hence, unlike in the case of T=123 K, the average structures can not be considered as representative configurations of high-temperature Mo(001) structures. A similar behavior has been reported also by Wang et al. [17] in theoretical study employing classical force-field simulations.

The temperature dependent work function has been computed as a thermal average ($\langle \ldots \rangle$) by means of the ergodic hypothesis as follows:

$$\langle \phi \rangle = \lim_{\tau \to \infty} \frac{1}{\tau} \int_0^{\infty} dt\, \phi(t), \tag{5}$$

where τ is the total length of trajectory and $\phi(t)$ is the value of ϕ computed at the time t. The structures for the ϕ calculations have been sampled with a time increment of 0.5 ps and they were used to build an extended symmetric model containing nine layers and the same vacuum gap as the models used in the zero temperature calculations. As shown in Fig. 2, the extended model has been prepared from an MD structure by attaching the mirror image of four layers above the first layer with fixed atoms to the bottom of the slab. In order to obtain well converged results consistent with our static calculations, a 6×6×1 k-points

grid with approximately the same density of k-points as used in our static calculations has been employed in the work function calculations. Further details of the finite-temperature ϕ calculations are presented in Sec.SIV of the Supplemental Material [33]. It can be seen from Fig. 4 that ϕ decreases monotonically with T. This result is understandable because the surface reconstruction causing the increase of ϕ from 3.88 eV to 4.11 eV at T=0 K (see Tab. II), vanishes, on average, when T is increased above T_c (vide supra). Although the average structures obtained from MD at T=423 K and 623 K correspond to unreconstructed bulk-like termination, the values of ϕ computed for these temperatures (4.05 eV and 4.04 eV) are still significantly higher than that obtained for the relaxed p(1×1) surface at 0 K. This result is a consequence of the fact that every instantaneous structure in MD at T_2 and T_3 is very different from the p(1×1) structure as it exhibits some of the structural features, such as the shortening of the nearest neighbour Mo-Mo distances, typical for the reconstructed surfaces described in Sec. III A (see Fig.S1 in the Supplemental Material [33]). As mentioned above, the averaged structures from the MD correspond to terminations c$(5\sqrt{2} \times \sqrt{2})$R45° (123 K) and p$(1 \times 1)$ (423 K and 623 K) and the values of ϕ computed for these averaged structures (4.11 eV, 3.87 eV, and 3.87 eV for T_1, T_2, and T_3, respectively) are indeed very close to the corresponding results obtained in relaxations.

C. Zero and finite temperature simulations of Mo(110)

As a further demonstration of the role of atomic displacement in the work function dependence on T, let us consider the Mo(110) surface (see Fig. 1(f)) which does not undergo any reconstruction. Compared to the surface (001), the particle density of atoms in the first layer is $\sqrt{2}$ higher. Due to the stronger in-plane and inter-plane interactions between atoms, the (110) surface undergoes a significantly weaker relaxation of interlayer distances compared to the slab (001) (see Tab. I) and it is also significantly more stable, as evident from the value of computed γ, which is 0.36 J/m^2 lower than that for the slab (001) with its most stable termination. All these results are in a good agreement with previous theoretical reports [8, 12, 34], see Tab. I and II. The value of ϕ computed upon relaxation of a nine-layers model is 4.54 eV, i.e. 0.66 eV higher than that for the unreconstructed (001) surface. The MD simulations have been performed for T=123 K, 423 K, and 623 K with a structural model and simulation setting analogous to those used in the MD simulations of Mo(001).

Unlike in the (001) surface, the RDF computed for the first and the second Mo layers are very similar in shape and the peaks are centered at expected bulk-like positions (see Fig. 5). The large broadening of the nearest neighbor peaks observed in the case of Mo(001) at 423 K and 623 K is not observed in the case of Mo(110) and hence not only average but also every instantaneous structure of Mo(110) is rather close to the ideal bulk-like termination (see animation Mo110_423K.mpg provided as Supplemental Material [33]). Clearly, this behavior is a consequence of a limited atomic motion due to the high particle density in Mo(110). As shown in Fig. 4, the finite temperature work function (ϕ=4.55 eV (123 K), 4.56 eV (423 K), and 4.56 eV (623 K)) determined in the same way as in the case of Mo(001) takes almost the same value, irrespective of T, as in our zero temperature calculations (4.54 eV). This result is perfectly in line with our results for Mo(001) suggesting that thermally induced displacements of surface atoms strongly affect the value of work function, and it is also consistent with the result of theoretical analysis of Kiejna [3] suggesting that the absolute value of the thermal coefficient of work function for a given metal decreases with an increase of the packing density in the plane.

IV. CONCLUSIONS

In summary, MD simulations and relaxations based on first-principles DFT reproduced correctly the observed surface phase transition of Mo(001) induced by temperature. The related structural changes occurring mainly in the first surface layer give rise to significant variation of work function. At low temperature (123 K), at which a stable reconstruction pattern is formed, the work function is found to increase by 0.23 eV compared to relaxed unreconstructed surface. With increasing temperature (423 K and 623 K), the stable reconstruction pattern vanishes and the average high-temperature structures correspond to perfect bulk-like termination. Consequently, the work function decreases but this decrease is reduced by the fact that the instantaneous structures formed at 423 K and 623 K still posses some of the structural features observed in the reconstructed patterns. In the case of the surface Mo(110), in which the surface reconstruction does not occur due to high surface particle density hindering the thermal atomic motion, the values of ϕ computed for T=123 K, 423 K, and 623 K are close to that for the zero-temperature structure. This result is consistent with the previous theoretical analysis of Kiejna [3] who correlated the absolute

value of the thermal coefficient of work function with the packing density of the surface, and it serves as a further demonstration of important role of thermally induced atomic displacements in the work function variation. The simulation protocol developed within this work will be applied in our future work to study cesiated Mo surfaces and the effect of interaction of Cs adsorbed on Mo with small molecules from the impurities originating from the background pressure of 10-6 mbar, which are the applications relevant for the development of effective H^- sources for the needs of future nuclear fusion devices.

ACKNOWLEDGMENTS

This work has been carried out within the framework of the EUROfusion Consortium and has received funding from the Euratom research and training programme 2014-2018 under Grant Agreement No. 633053. The views and opinions expressed herein do not necessarily reflect those of the European Commission. We are grateful to the Slovak Research and Development Agency under the contract No. APVV-15-0105 for the support. Calculations were performed using supercomputing infrastructure of Computing Center of the Slovak Academy of Sciences acquired in projects ITMS 26230120002 and 26210120002 supported by the Research and Development Operational Program funded by the ERDF.

[1] N. W. Ashcroft and N. D. Mermin, in Solid state physics (Saunders, Philadelphia, 1976) p. 354.

[2] K. I. Ibragimov and V. A. Korol̆kov, Inorg. Mater. **37**, 567 (2001).

[3] A. Kiejna, Surf. Sci. **178**, 349 (1986).

[4] P. Franzen, H. Falter, E. Speth, W. Kraus, M. Bandyopadhyay, A. Encheva, U. Fantz, T. Franke, B. Heinemann, D. Holtum, C. Martens, P. McNeely, R. Riedl, A. Tanga, and R. Wilhelm, Fus. Eng. Des. **74**, 351 (2005), proceedings of the 23rd Symposium of Fusion Technology.

[5] U. Fantz, P. Franzen, and D. Wuenderlich, Chem. Phys. **398**, 7 (2012).

[6] S. R. Chubb, E. Wimmer, A. J. Freeman, J. R. Hiskes, and A. M. Karo, Phys. Rev. B **36**, 4112 (1987).

[7] M. Methfessel, D. Hennig, and M. Scheffler, Phys. Rev. B **46**, 4816 (1992).

[8] J. G. Che, C. T. Chan, W.-E. Jian, and T. C. Leung, Phys. Rev. B **57**, 1875 (1998).

[9] A. Kiejna and R. M. Nieminen, Phys. Rev. B **66**, 085407 (2002).

[10] A. Kiejna and R. Nieminen, Phys. Rev. B **69**, 235424 (2004).

[11] S. D. Waele, K. Lejaeghere, M. Sluydts, and S. Cottenier, Phys. Rev. B **94**, 235418 (2016).

[12] M. Chen, J. Roszell, E. V. Scoullos, C. Riplinger, B. E. Koel, and E. A. Carter, J. Phys. Chem. B **120**, 6110 (2016).

[13] T. E. Felter, R. A. Barker, and P. J. Estrup, Phys. Rev. Lett. **38**, 1138 (1977).

[14] E. Hulpke and D. M. Smilgies, Phys. Rev. B **43**, 1260 (1991).

[15] D. M. Smilgies, P. J. Eng, and I. K. Robinson, Phys. Rev. Lett. **70**, 1291 (1993).

[16] M. L. Hildner, R. S. Daley, T. E. Felter, and P. J. Estrup, Phys. Rev. B **52**, 9050 (1995).

[17] C. Z. Wang, E. Tosatti, and A. Fasolino, Phys. Rev. Lett. **60**, 2661 (1988).

[18] L. D. Roelofs and S. M. Foiles, Phys. Rev. B **48**, 11287 (1993).

[19] H. Haas, C. Wang, K. Ho, M. Fähnle, and C. Elsässer, Surf. Sci. **457**, L397 (2000).

[20] G. Kresse and J. Hafner, Phys. Rev. B **48**, 13115 (1993).

[21] G. Kresse and J. Hafner, J. Phys. Condens. Matter **6**, 8245 (1994).

[22] G. Kresse and J. Furthmüller, Comp. Mater. Sci. **6**, 15 (1996).

[23] G. Kresse and J. Furthmüller, Phys. Rev. B **54**, 11169 (1996).

[24] P. E. Blöchl, O. Jepsen, and O. K. Andersen, Phys. Rev. B **49**, 16223 (1994).

[25] G. Kresse and D. Joubert, Phys. Rev. B **59**, 1758 (1999).

[26] J. P. Perdew, K. Burke, and M. Ernzerhof, Phys. Rev. Lett. **77**, 3865 (1996).

[27] W. H. Press, S. A. Teukolsky, W. T. Vetterling, and B. P. Flannery, Numerical Recipes: The Art of Scientific Computing (3rd Edn.) (Cambridge Univ. Press, New York, 2007) pp. 515–520.

[28] F. D. Murnaghan, P. Natl. Acad. Sci. USA **30**, 244 (1944).

[29] M. E. Straumanis and C. L. Woodward, Acta Cryst. A **27**, 549 (1971).

[30] N. D. Lang and W. Kohn, Phys. Rev. B **3**, 1215 (1971).

[31] H. C. Andersen, J. Chem. Phys. **72**, 2384 (1980).

[32] D. Frenkel and B. Smit, Understanding molecular simulation: from algorithms to applications (Academic press: San Diego, 2002) pp. 69–71.

[33] See supplemental material at [URL will be inserted by publisher] for structural details of relaxed slab models, convergence tests, details on finite-temperature work function calculations, and animations showing Mo(001) and Mo(110) at various T.

[34] S. De Waele, in Thesis (University of Ghent, 2015).

[35] J.-Y. Lee, M. Punkkinen, S. Schönecker, Z. Nabi, K. Kádas, V. Zólyomi, Y. Koo, Q.-M. Hu, R. Ahuja, B. Johansson, J. Kollár, L. Vitos, and S. Kwon, Surf. Sci. **674**, 51 (2018).

[36] A. E. Carlsson, Phys. Rev. B **44**, 6590 (1991).

[37] G. N. Derry, M. E. Kern, and E. H. Worth, J. Vac. Sci. Technol. A **33**, 060801 (2015).

[38] G. Makov and M. C. Payne, Phys. Rev. B **51**, 4014 (1995).

[39] `https://www.iter.org`.

[40] Y. S. Touloukian, in Thermophysical Properties of Matter, Vol. 12 (IFI/Plenum, New York, 1975).

TABLE I. Average relative change in separation between layers m and n ($\Delta_{m,n}$) of relaxed slab models of Mo(001) and Mo(110) with different surface terminations. The values reported in previous theoretical work of Che et al. [8] are given in parenthesis.

Surface	Termination	$\Delta_{1,2}$ (%)	$\Delta_{2,3}$ (%)	$\Delta_{3,4}$ (%)	$\Delta_{4,5}$ (%)
Mo(001)	p(1 × 1)	−13.4 (−11.1)	3.7 (2.3)	−0.8 (−1.7)	0.2 (0.3)
	c($\sqrt{2} \times \sqrt{2}$)R45°	−8.5	1.2	0.2	−0.3
	c($3\sqrt{2} \times \sqrt{2}$)R45°	−10.2	2.6	−0.4	0.1
	c($5\sqrt{2} \times \sqrt{2}$)R45°	−9.7	2.1	−0.1	−0.1
	c($7\sqrt{2} \times \sqrt{2}$)R45°	−9.5	1.9	−0.1	−0.1
Mo(110)	p(1 × 1)	−5.0 (−4.3)	0.7 (−0.2)	0.1 −0.4	0.0 (−0.7)

TABLE II. Surface energy (γ) and work function (ϕ) computed for diverse terminations of Mo(001) and for the unreconstructed Mo(110) at T=0 K. Previous theoretical results of Chen et al. [12], De Waele [34], and Lee at al. [35] obtained using the same DFT approximation as employed in this work are given in parenthesis.

Surface	Termination	γ (J/m^2)	ϕ (eV)
Mo(001)	Exp.	n.a.	4.46±0.11 [37]
	p(1 × 1) (unrelaxed)	3.524	3.92
	p(1 × 1) (relaxed)	3.259 (3.29 [12],3.19 [34], 3.15 [35]))	3.88 (3.84 [34])
	c($\sqrt{2} \times \sqrt{2}$)R45°	3.201	4.12
	c($3\sqrt{2} \times \sqrt{2}$)R45°	3.208	4.11
	c($5\sqrt{2} \times \sqrt{2}$)R45°	3.196	4.11
	c($7\sqrt{2} \times \sqrt{2}$)R45°	3.199	4.10
Mo(110)	Exp.	n.a.	4.92±0.05 [37]
	p(1 × 1)	2.833 (2.81 [12],2.77 [34], 2.73 [35]))	4.54 (4.52 [34])

TABLE III. Average in-plane displacements δ_n (see eq. 4) computed for five symmetry non-equivalent layers (n) of slab models of Mo(001) with different surface terminations.

Termination	δ_1 (Å)	δ_2 (Å)	δ_3 (Å)	δ_4 (Å)	δ_5 (Å)
c($\sqrt{2} \times \sqrt{2}$)R45°	0.252	0.012	0.001	0.000	0.007
c($3\sqrt{2} \times \sqrt{2}$)R45°	0.195	0.028	0.001	0.005	0.003
c($5\sqrt{2} \times \sqrt{2}$)R45°	0.227	0.023	0.009	0.005	0.003
c($7\sqrt{2} \times \sqrt{2}$)R45°	0.224	0.019	0.007	0.003	0.005

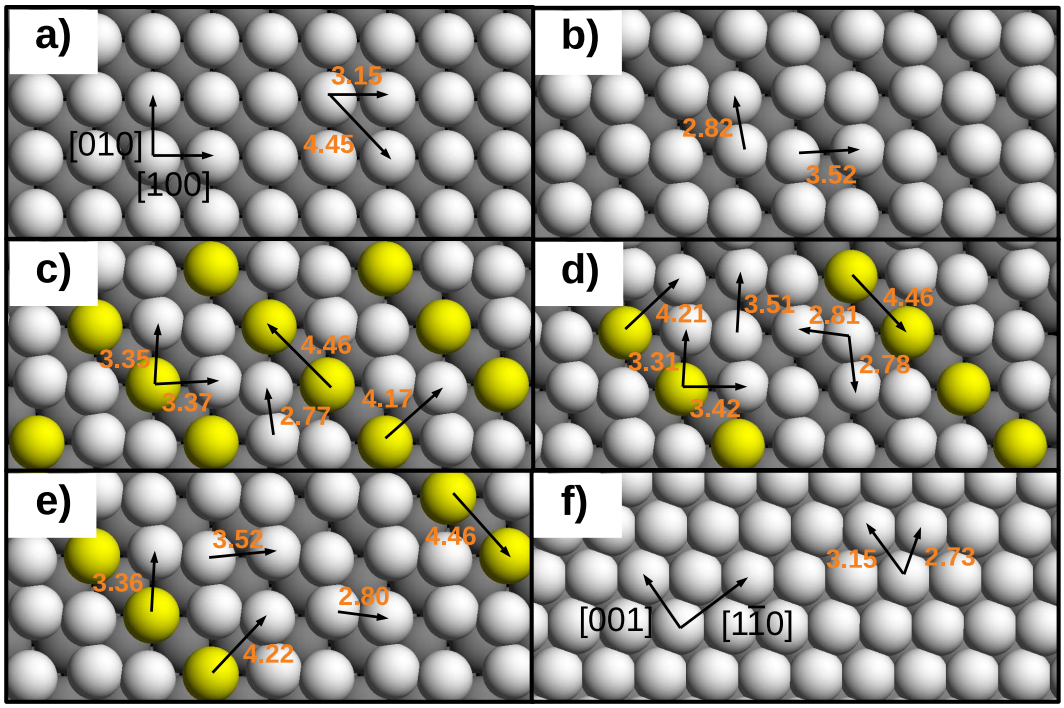

FIG. 1. Top view of the Mo(001) surface with terminations (a) p(1 × 1), (b) c($\sqrt{2} \times \sqrt{2}$), (c) c($3\sqrt{2} \times \sqrt{2}$)R45°, (d) c($5\sqrt{2} \times \sqrt{2}$)R45°, and (e) c($7\sqrt{2} \times \sqrt{2}$)R45°, and (f) the Mo(110) surface with the p(1 × 1) termination. The atoms forming the misfit rows in the case of some reconstructed surfaces are colored yellow while a dark gray color indicates atoms in the second layer. Selected interatomic distances (Å) between atoms in the first layer are shown.

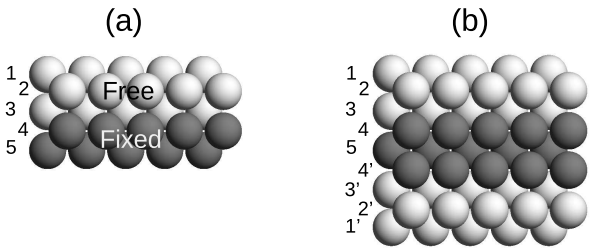

FIG. 2. Side views of the slab model of Mo(001) used in MD simulations (a), and in the finite-temperature work function calculations (b). The positions of atoms in two bottommost layers 4 and 5 of the slab (a) were fixed whereas the atoms in the layers 1−3 were free to move. The model (b) is constructed from (a) by attaching the mirror images of layers 1-4 (labeled as 1'-4') to the bottom of the slab whereby the mirror plane was chosen to be parallel with (001) and to cross the center of the layer 5.

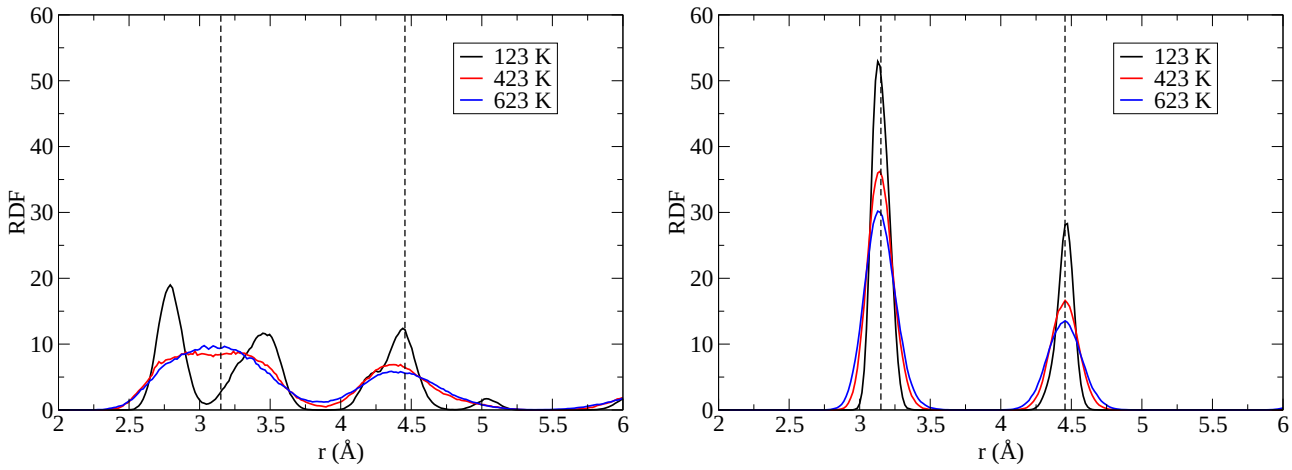

FIG. 3. Radial distribution functions computed for the first (left) and the second (right) layer of the surface Mo(001) at three different temperatures. Vertical dashed lines indicate the nearest ($r = a$) and the next-nearest neighbor ($r = \sqrt{2}a$) distances within the (001) planes of bulk Mo (cf. Fig. 1(a)).

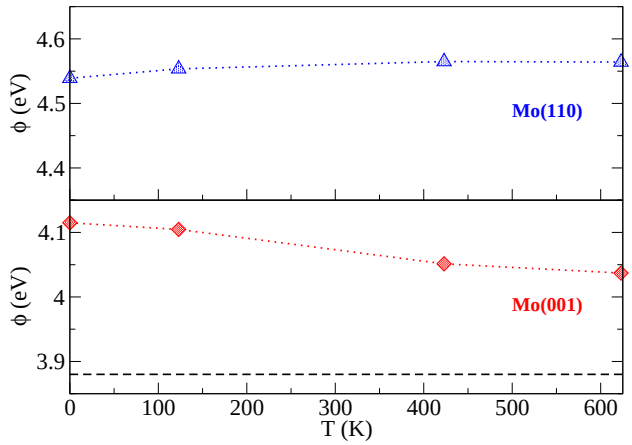

FIG. 4. Work function of Mo(001) and Mo(110) computed using MD simulations for different temperatures.

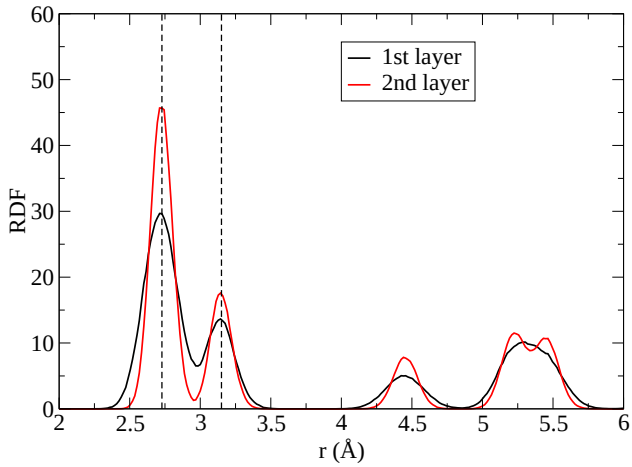

FIG. 5. Radial distribution functions computed for the first and the second layer of the surface Mo(110) at T=423 K. Vertical dashed lines indicate the nearest ($r = (\sqrt{3}/2)a$) and the next-nearest ($r = a$) neighbor distances within the (110) planes of bulk Mo (cf. Fig. 1(f)).